ELSEVIER

Journal of Alloys and Compounds 293–295 (1999) 501–507

Journal of ALLOYS AND COMPOUNDS

Structural investigation and solid-H_2 reaction of Mg_2Ni rich nanocomposite materials elaborated by mechanical alloying

M. Abdellaoui[a,*], D. Cracco[b], A. Percheron-Guegan[b]

[a]*National Institute of Research & Physic-chemistry analyses 1, Rue Jawhar Sekelli, MENZEH 7, Tunis 1004, Tunisia*
[b]*Laboratoire de Chimie Métallurgique des Terres Rares Glvt, 2-8, rue Henri Dunant, F- 94320 Thiais Cedex, France*

Abstract

Using a planetary ball mill and starting from a mixture of Mg and Ni with an atomic ration of 2:1, we have successfully elaborated a nanocomposite material formed by the Mg_2Ni phase in high proportion, some residual Ni and an amorphous phase. The synthesis of this composite proceeded at milling intensities 7 and 10, corresponding respectively to 3.5 and 10 W g^{-1} shock power, respectively after 18 and 4 h. The best hydrogen absorption capacity reported, 3.75 H $mole^{-1}$ (3.53 wt.%), is for the composite synthesized for 24 h at 3.5 W g^{-1} shock power.

Keywords: Mg–Ni nanocomposite materials; Mechanical alloying; Hydrogen absorption–desorption properties

1. Introduction

The reversible absorption of hydrogen by some intermetallic compounds in order to form some metallic hydrides was discovered in the 1950's. Recently, the potential use of these materials as reversible high density hydrogen gas storage and as electrode in the alkaline Ni–hydride accumulator rose many interests.

Magnesium has a high hydrogen absorption capacity. Nevertheless, the hydrogen absorption–desorption process needs high temperatures (>600 K) with very low kinetics. So, Mg rich intermetallic alloys were investigated in order to determine the optimum composition leading to the best reversible hydrogen absorption properties. Mg_2Ni is the most intensively studied due to its low specific weight and its low cost [1]. The magnesium absorption kinetics are improved by the Ni addition, because of its good catalytic activity [2].

It is well established that, in the metal–hydride systems, the improving of the hydrogen absorption properties such as the reduction of the activation time, the improvement in the kinetics of the reaction and the increase of the absorption capacity are strongly dependent of the surface area and the particle size of the material. In fact, the defects created on the surface of the mechanically synthesized material, during the absorption–desorption cycles, can play the role of nucleation sites for the formation of the Mg_2Ni hydride [3]. On the other hand, it is well known that mechanical alloying induces an increase of the specific surface area and of the defect density on the surface as well as in the volume of the material. The mechanical alloying process is then intensively used as a process for the formation of Mg_2Ni rich nanocomposite material for further hydriding. Moreover, mechanical alloying was used successfully to elaborate some hydrides in situ [4–6].

The hydrogen absorption properties of Mg_2Ni alloys synthesized by mechanical alloying, starting from mixtures of elementary powders [5–7] as well as the milling effects on the already alloyed Mg_2Ni have been reported these last years [8,9]. Using the Fritsch pulverisette P5 planetary ball mill, Huot et al. [5] synthesized the intermetallic Mg_2Ni when starting with a mixture of Mg and Ni in an atomic ratio 2:1, under an argon atmosphere. The authors [5] showed that the stationary state was reached after 22 h. Singh et al. [7] elaborated the Mg_2Ni phase with some free Ni when starting from the same mixture but when using an attriteur mill. The stationary state resulted after about 100 h of ball milling. The hydrogen absorption capacities reported, respectively, by Singh et al. [7] and Song [3] were 3.2 and 3.22 wt.%.

So, the purpose of this paper is the optimization of the mechanical alloying process in order to synthesize, with the smallest mechanical alloying duration, some Mg_2Ni

*Corresponding author. Tel.: +216-1-750-819; fax: +216-1-238-133.

0925-8388/99/$ – see front matter
PII: S0925-8388(99)00475-2

rich nanocomposite material with no residual Mg, having the best hydrogen absorption properties.

2. Experimental procedure

The mechanical alloying (MA) processes were carried out using the P7 Fritsch planetary ball mill and a specially designed machine called G7 [10], which allows to control the disc and the vial effective rotation speeds during the mechanical alloying process. A 5 g amount of a mixture of pure Mg (metallic Mg, 99.6%) and pure Ni (99.9%) with an atomic proportion of 2:1 were introduced into a cylindrical tempered steel container of 45 ml capacity. Each container was loaded with five balls (Φ=15 mm, m=14 g or Φ=12 mm, m=13 g). This procedure was performed in a glove box filled with purified argon. The containers were sealed in the glove box with an elastomer Taurus ring allowing perfect air tightness. Thus, the milling processes proceeded in a stationary argon atmosphere.

After continuous milling, a small amount of the mechanically alloyed powder was extracted from the container for further X-ray investigations. X-ray diffraction (XRD) patterns were obtained using a ($\theta-2\theta$) Philips diffractometer with Cu Kα radiation. A numerical method – the ABFfit program [11] – was used in order to analyze the XRD patterns and to obtain the position and the full-width at half height (FWHH) of the various peaks. In this work, the Gaussian function seems to be the suitable function for the XRD pattern analysis as have been used in previous works [12–18].

The effective particle sizes (hereafter referred to as Φ) were calculated from Scherrer's expression. The morphological characterization of the synthesized samples were carried out using a Jeol-JSM-840 scanning electron microscope. The pressure–composition (P–C) isotherms were measured at 553 K and 25 bar initial pressure, with Sievert's method. Before measuring the P–C isotherm, the sample was sufficiently activated by a thermal treatment: 553 K during a few hours under primary vacuum, followed by three absorption–desorption cycles.

3. Experimental results

3.1. Relationship between the end product structure and the alloying conditions

To check the possibility of alloying at low injected shock power, two samples were elaborated using Pulverisette 7 set at intensity 7 (disc rotation speed (Ω)=510 rpm and vial rotation speed (ω)=1020 rpm) during 24 h. The milling was accomplished by means of five balls weighing 13 g each. All samples were obtained starting from a mixture of Mg and Ni in an atomic ratio 2:1. The

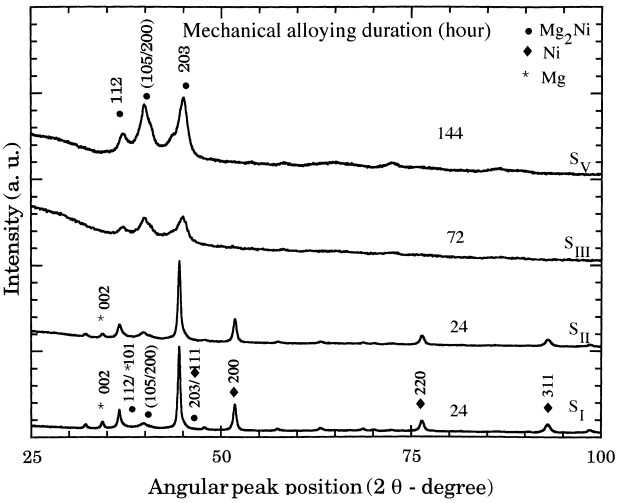

Fig. 1. X-ray diffraction (XRD) patterns corresponding to samples S_I, S_{II}, S_{III} and S_V (the milling conditions are indicated in Table 1).

first sample S_I has 10 g weight whereas S_{II} was weighing only 5 g. Fig. 1 gives the XRD patterns corresponding to samples S_I and S_{II}. The XRD pattern analyses revealed that the sample S_I contained the Mg_2Ni phase in moderate proportion with residual Ni and Mg components. The increase of the injected shock power per gram, by reduction of the sample mass to one half while keeping the milling duration equal to 24 h, induced formation of a nanocomposite containing Mg_2Ni and elemental Ni in high proportion with some traces of metallic Mg (Table 1).

As our aim in this study is the elaboration of some Mg_2Ni rich nanocomposite materials, free of residual Mg, the G7 planetary ball mill was used to mill during 72 and 144 h, respectively sample S_{III} and S_V. The vial (ω) and the disc (Ω) rotation speeds were, respectively, equal to 508 and 1000 rpm. The powder mass as well as the number of balls remained the same as for S_{II}. XRD patterns analysis showed that both samples only contained Mg_2Ni and an amorphous phase with no remaining elemental Mg or Ni (Table 1).

Based on results of Abdellaoui et al. [10,19], the injected shock power per gram is the unique physical parameter governing the stationary state structure. Therefore, we were interested in increasing the injected shock power value in order to synthesize the desired material with smaller milling duration. The injected shock power can be increased by increasing the ball mass while keeping all the other parameters unchanged. So, new balls with 15 mm diameter and 14 g mass were used instead of the 12 mm diameter and 13 g mass ones used previously. The optimal milling time to obtain a nanocomposite material free of metallic Mg is determined by decreasing the synthesis duration, starting from a milling duration of 48 h, until the appearance of some crystalline peaks characteristic of the presence of some traces of the metallic Mg.

Fig. 2 gives the XRD patterns corresponding to samples

Table 1
Synthesis conditions and analysis results of the X-ray diffraction (XRD) patterns corresponding to samples elaborated by the P7 ball mill set at intensity 7 (Ω=510 rpm, ω=1020 rpm) and G7 ball mill (Ω=508 rpm, ω=1000 rpm) starting from powder mixtures of Mg and Ni in atomic proportions of 2:1, the five balls used have 13 g mass and 12 mm diameter, the injected shock power per gram of powder, expressed in watt per gram (W g^{-1}), as well as the total shock power injected by the five balls in the total quantity of powders, expressed in watt (W), are included in the table

Sample	Ball milling conditions: m [g] Δt [h]	· Total shock power [W] · Energy (J/hit) · Total shock frequency [Hz]	Phases (lattice parameters, [Å])	Grain size [Å]
S_I	· P7/7,		Mg (3.20, 5.21)	172
	· m=10,		Ni (3.53)	152
	· Δt=24	9.905	Mg_2Ni (5.21, 14.21)	82
S_{II}	· P7/7,	0.089	Mg (3.20, 5.15)	123
	· m=5	111.05	Ni (3.54)	196
	· Δt=24		Mg_2Ni (5.21, 14.01)	74
S_{III}	· G7,		Mg_2Ni (5.17, 13.8)	75
	· m=5		Amorphous (2.18)	–
	· Δt=72	10.135		
S_V	· G7,	0.0927	Mg_2Ni (5.24, 13.0)	87
	· m=5	109.3	Amorphous (2.14)	–
	· Δt=144			

S_{VII}, S_{VIII}, S_{XIII}, S_{XIV} and S_{XV}, milling conditions and structural parameters are indicated in Table 2. The XRD patterns analyses revealed that for milling duration equal to 48 (S_{VIII}), 24 (S_{VII}) and 18 (S_{XIV}) h, the material contained three phases: the Mg_2Ni phase and an amorphous phase in high proportions with some residual Ni. The decrease of the alloying duration until 15 h (S_{XV}) did not allow a full consumption of all the initial quantity of the metallic Mg and some weak intensity peaks relative to the residual Mg remained in the XRD pattern (Fig. 2). So, at milling intensity 7 (injected shock power=3.5 W g^{-1}), the optimal ball milling duration leading to the formation of Mg_2Ni rich nanocomposite without residual Mg, will be located between 15 and 18 h.

We previously reported [20] that the intermediary state depends on the accumulated energy (expressed in W h g^{-1}) given by the product of the injected shock power (W g^{-1}) and the milling duration. Consequently, the increase of the injected shock power allows the formation of the same intermediary state but at lesser alloying duration. Based on the accumulated energy equation, when using the milling intensity 10 (injected shock power=10 W g^{-1}), the Mg_2Ni rich nanocomposite materials, free of residual Mg, can be obtained for alloying duration less than 8 h. Fig. 3 gives the XRD patterns corresponding to samples S_{XI}, S_{XVI}, S_{XVII}, S_{XVIII} and S_{XIX}, milling conditions are indicated in Table 3. The XRD patterns analyses revealed that for milling duration equal to 13 (S_{XIX}) and 8 (S_{XI}) h, the elaborated material contained only two phases: the Mg_2Ni phase and an amorphous phase. Whereas the samples S_{XVII} (6 h) and S_{XVI} (4 h) contained three phases: namely the Mg_2Ni phase, the residual Ni and an amorphous phase. When decreasing the ball milling duration, to 2 h (S_{XVIII}), the Ni and Mg remained at the elementary state and no reaction, even partial, occurred. So, 4 h could therefore be considered as the optimal alloying time at milling intensity 10.

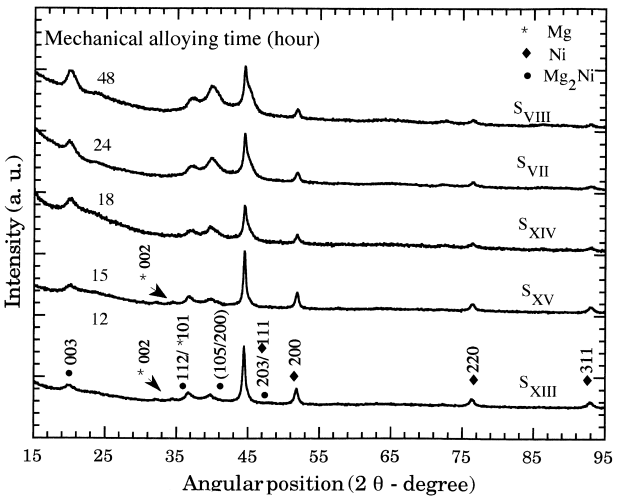

Fig. 2. X-ray diffraction (XRD) patterns corresponding to samples S_{VIII}, S_{VII}, S_{XIV}, S_{XV} and S_{XIII} (the milling conditions are indicated in Table 2).

3.2. Morphological properties

Fig. 4a and b give SEM images in secondary electron mode of, respectively, the S_{III} sample (Table 1) and the S_{VII} sample (Table 2). The alloyed particles (formed by an assembly of nanocrystalline grains, which size is equal to the coherence domain size given by the XRD patterns analyses) showed heterogeneous distributions. Their sizes varied from a few μm (2–3) to many μm (20–25).

3.3. Solid-H_2 reaction properties

After being submitted to an activation process, the samples were maintained in a secondary vacuum at 280°C during 1 h. After that, the P–C desorption isotherms were determined at the same temperature starting from a pres-

Table 2
Synthesis conditions and analysis results of the XRD patterns corresponding to samples elaborated by the P7 ball mill set at intensity 7 ($\Omega = 510$ rpm, $\omega = 1020$ rpm) starting from 5 g of powder mixtures of Mg and Ni in atomic proportions of 2:1, the five balls used have 14 g mass and 15 mm diameter, the injected shock power per gram of powder, expressed in watt per gram (W g^{-1}), as well as the total shock power injected by the five balls in the total quantity of powders, expressed in watt (W), are included in the table

Sample	Milling duration: Δt [h]	· Total shock power [W] · Energy (J/hit) · Total shock frequency [Hz]	Phases (lattice parameters, [Å])	Grain size [Å]
S_{XIII}	$\Delta t = 12$		Mg_2Ni (5.3, 13.2)	71
			Mg (3.21, 5.21)	151
			Ni (3.53)	170
			Amorphous (2.3)	–
S_{XV}	$\Delta t = 15$		Mg_2Ni (5.3, 13.3)	71
			Mg (3.24, 5.19)	138
			Ni (3.52)	62 and 173
			Amorphous (2.3)	–
		17.245		
S_{XIV}	$\Delta t = 18$	0.1627	Mg_2Ni (5.3, 13.2)	76
		106	Ni (3.51)	129
			Amorphous (2.3)	–
S_{VII}	$\Delta t = 24$		Mg_2Ni (5.3, 13.2)	89
			Ni (3.52)	115
			Amorphous (2.2)	–
S_{VIII}	$\Delta t = 48$		Mg_2Ni (5.2, 13.2)	72
			Ni (3.52)	126
			Amorphous (2.2)	–

sure of 25 bar. Fig. 5a and b show the P–C desorption curves (a) for the samples S_{III}, S_{VII}, S_{VIII} and S_{XIV} and (b) for the samples S_{XI}, S_{XVI}, and S_{XVII}. The sample S_{VII} had the best absorption capacity with 3.5 wt.% (3.75 H mol^{-1}). All the other samples had an absorption capacity around 3.25 wt.% (3.5 H mol^{-1}). S_{VII}, S_{VIII} and S_{XIV} showed a 0.3 MPa plateau pressure, whereas S_{XI}, S_{XVI} and S_{XVII} showed a lower plateau pressure of 0.21 MPa.

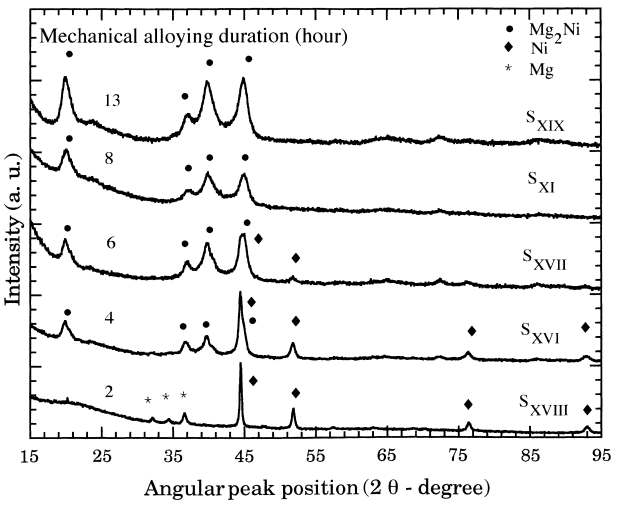

Fig. 3. X-ray diffraction (XRD) patterns corresponding to samples S_{XIX}, S_{XI}, S_{XVII}, S_{XVI} and S_{XVIII} (milling conditions are indicated in Table 3).

4. Discussion

4.1. Mechanically alloyed material microstructure versus the alloying conditions

Fig. 6 shows a (Alloying duration–Injected shock power) far from equilibrium phase diagram for the ball milled Mg–Ni powder mixture (2:1 atomic proportion). Based on this phase diagram, we noted that, depending on the injected shock power and the alloying duration values, mechanical alloying induced the formation of one of the following nanocomposite material: (a) Mg+Ni, (b) Mg_2Ni+Mg+Ni, (c) Mg_2Ni+Mg+Ni+Amorphous, (d) Mg_2Ni+Ni+Amorphous and (e) Mg_2Ni+Amorphous.

Using ball milling conditions corresponding to a low injected shock power of 2 W g^{-1}, the formation of the Mg_2Ni phase began at 24 h milling duration. An increase of the alloying duration up to 72 h induced the total transformation of the initial elementary powders of Mg and Ni into the Mg_2Ni phase, partially amorphous. The increase of the injected shock power up to 3.5 W g^{-1}, led to the formation of a nanocomposite, mixture of the Mg_2Ni phase and an amorphous phase with residual Mg and Ni, for alloying duration less than 15 h. For higher alloying duration, mechanical alloying led to the consumption of all the residual Mg and the formation of a nanocomposite only containing the Mg_2Ni phase and an amorphous phase with some residual Ni. When the injected shock power reached a high value of 10 W g^{-1}, initial Mg and Ni powders

Table 3
Synthesis conditions and analysis results of the XRD patterns corresponding to samples elaborated by the P7 ball mill set at intensity 10 (Ω=726 rpm, ω=1452 rpm) starting from 5 g of mixtures of Mg and Ni powders in atomic proportions of 2:1, the five balls used have 14 g mass and 15 mm diameter, the injected shock power per gram of powder, expressed in watt per gram (W g^{-1}), as well as the total shock power injected by the five balls in the total quantity of powders, expressed in watt (W), are included in the table

Sample	Milling duration: Δt [h]	· Total shock power [W] · Energy (J/hit) · Total shock frequency [Hz]	Phases (lattice parameters, [Å])	Grain size [Å]
S_{XVIII}	Δt=2		Mg (3.21, 5.21)	128
			Ni (3.52)	55 and 186
S_{XVI}	Δt=4		Mg_2Ni (5.25, 13.25)	115
			Ni (3.52)	47 and 146
			Amorphous (2.3)	–
		49.82		
S_{XVII}	Δt=6	0.33	Mg_2Ni (5.22, 13.42)	87
		151	Ni (3.51)	105
			Amorphous (2.3)	–
S_{XI}	Δt=8		Mg_2Ni (5.23, 13.21)	56
			Amorphous (2.1)	–
S_{XIX}	Δt=13		Mg_2Ni (5.22, 13.27)	60
			Amorphous (2.2)	–

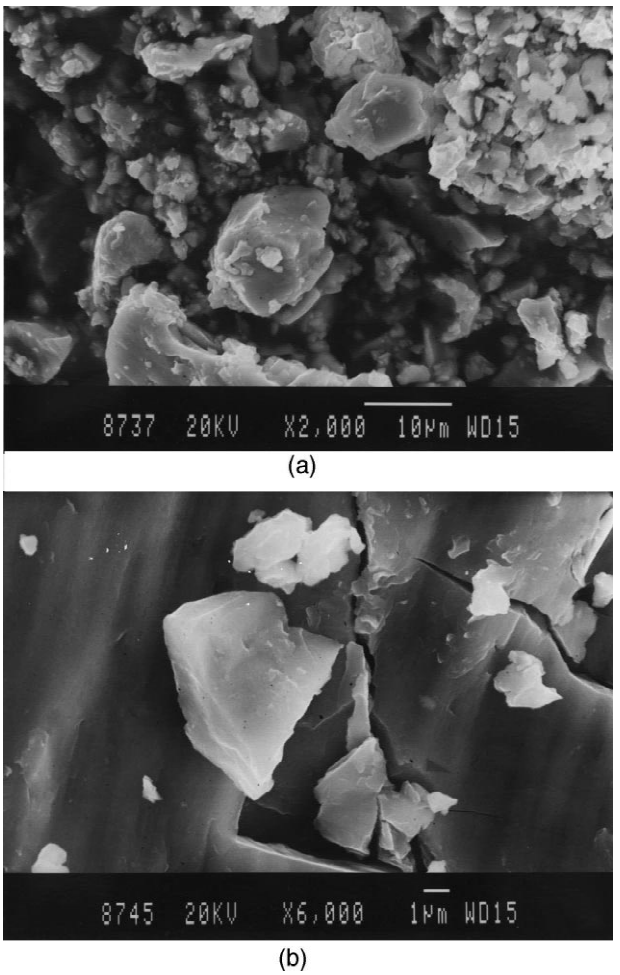

Fig. 4. SEM image, in secondary electron mode, of (a) the sample S_{III} and (b) the sample S_{VII}.

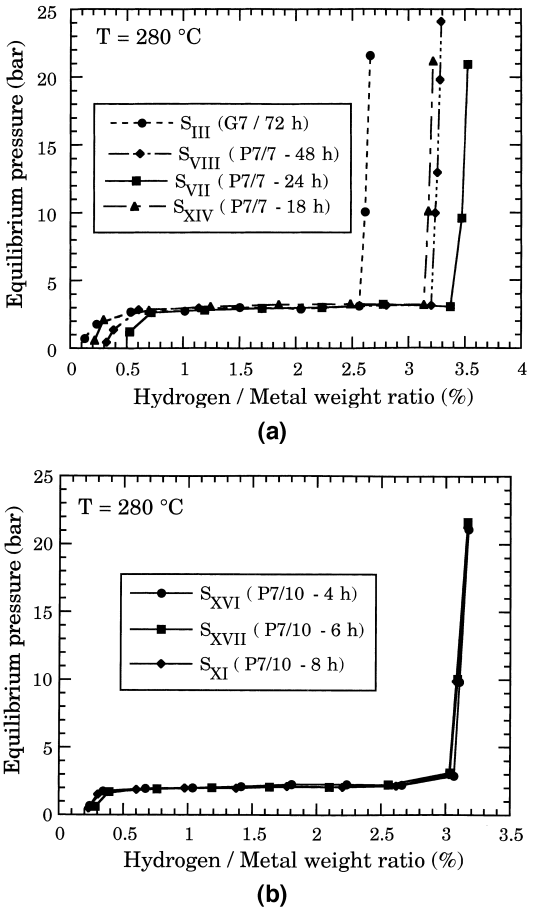

Fig. 5. Pressure–composition desorption curves, carried out at a temperature of 280°C and an initial pressure of 25 bar for (a) the samples S_{III}, S_{VII}, S_{VIII} and S_{XIV} and (b) for the samples S_{XI}, S_{XVI} and S_{XVII}, after being submitted to an activation process and maintained in a secondary vacuum at 280°C during 1 h.

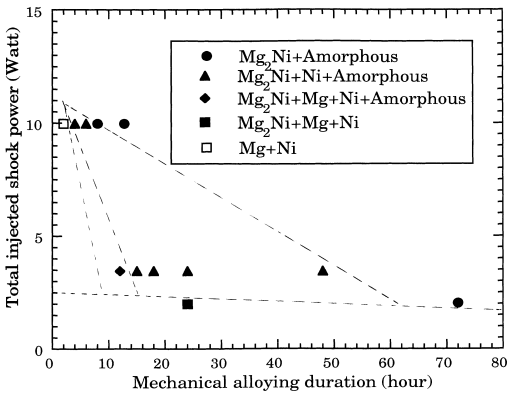

Fig. 6. (Alloying duration–Injected shock power) far from equilibrium phase diagram for the mechanically alloyed Mg–Ni powder mixtures (2:1 atomic proportion).

remained in the elementary state up to 2 h alloying duration but turned into a nanocomposite formed by the Mg_2Ni phase and an amorphous phase with some residual Ni after 4 h milling. For alloying duration higher than 6 h, mechanical alloying led to a nanocomposite only containing the Mg_2Ni phase and an amorphous phase free of the initial Mg and Ni components.

Based on these results, we showed that we could optimize the mechanical alloying process to form the Mg_2Ni rich nanocomposite material free of Mg, suitable for the reversible hydrogen absorption, at milling duration (4 h for 10 W g^{-1} injected shock power) shorter than those reported in Ref. [5] (22 h) or in Ref. [7] (100 h).

In our previous work [21], the formation kinetics of, respectively, the Mg_2Ni phase and the amorphous phase, at different injected shock powers have been studied. The formation kinetics of the intermetallic Mg_2Ni was shown by the variation of the Mg_2Ni (003) peak intensity to the Ni (200) peak intensity ratio, whereas, that of the amorphous phase was shown by the variation of the amorphous intensity to the Ni (200) peak intensity ratio. It had been concluded that for the injected shock power as low as 3.5 W g^{-1}, the formation kinetics of the Mg_2Ni phase and the amorphous phase were globally slow. They were shown to be stabilized after 24 h alloying duration, where the system reached its stationary state formed by the Mg_2Ni phase and the amorphous phase in high proportions with some residual Ni. Nevertheless, for the injected shock power as high as 10 W g^{-1}, the above mentioned formation kinetics were very fast. The two respective ratios increased very abruptly and particularly between 4 and 6 h alloying duration where the residual Ni still existed in the presence of the Mg_2Ni phase and the amorphous phase. After 8 h milling duration, the stationary state was formed by only the Mg_2Ni and the amorphous phase.

So, as reported in Refs. [10,19], we have newly showed that the higher the injected shock power, the higher the formation and the transformation kinetics of the intermediary phases. Similarly, we showed that, for the same milling duration, as the injected shock power increased, the end product state was more and more distinct from the thermodynamic equilibrium state. So, for example as can be shown in Fig. 6, for the 3.5 W g^{-1} injected shock power, we obtain the [Ni+Mg_2Ni+amorphous] nanocomposite material. However, for the 10 W g^{-1} injected shock power, we obtain the [Mg_2Ni+amorphous] nanocomposite material.

Now when keeping the injected shock power constant, if its value is higher than a critical one allowing the desired phase transition, the formation of this desired phase will begin after a given milling duration, even this milling duration is prolonged, as we have reported in our previous work [20]. So, as it can be seen in Fig. 6, we have the formation of a nanocomposite material formed by the Mg_2Ni and the amorphous phases for a milling duration equal at least to 72 h for an injected shock power of 2 W g^{-1}. This value of injected shock power is then assumed to be higher than the critical value allowing the formation of this nanocomposite material.

4.2. Properties of the H_2 absorption by the Mg_2Ni rich nanocomposite material

As shown in Fig. 5a, the hydrogen absorption capacity increased with alloying duration up to 24 h (3.75 H mol^{-1}) and then decreased for higher alloying duration. This alloying duration corresponds to the formation of a Mg_2Ni rich nanocomposite material with some residual Ni in addition to an amorphous phase. We assume that during the mechanical alloying process, defects are created and surface area is increased. Such defects serve as nucleation sites for the hydride formation and contribute to facilitate the hydrogen absorption [7]. Then, for higher alloying duration, milling may induce material hardening, severe lattice distortions and amorphization, which do not enable the occupation of the Mg_2Ni lattice interstitial sites by the hydrogen atoms and therefore induce a decrease in the hydrogen absorption capacity. The sample S_{III}, synthesized after 72 h alloying (Table 1) and containing only the Mg_2Ni phase and an amorphous phase, had a hydrogen absorption capacity less than those of the S_{XIV}, S_{VII} and S_{VIII} samples (Table 2), even if the injected shock power was smaller (2 W g^{-1} instead of 3.5 W g^{-1}). At this injected shock power, the high lattice distortion and material hardening due to the high milling duration, will account for this behavior.

Regarding the injected shock power of 10 W g^{-1} (samples S_{XI}, S_{XVI}, S_{XVII}), the absorption capacity was constant with milling time. This may be explained by the fact that amorphization takes place quicker than with an injected shock power of 3.5 W g^{-1}. So, we assume that the increase of the hydrogen absorption capacity due to the increase of defects and surface area would then be annihilated by the amorphization, lattice distortion and

material hardening. It is extremely interesting to note that the plateau pressure of these three samples was smaller than the one of S_{XIV}, S_{VII} and S_{VIII}. This means that the increase of the injected shock power induce the decrease of the mean grain size which may induce the decrease of the standard free energy of the hydride formation (ΔG_T^0). The decrease of this standard free energy induce, when aging at constant temperature, the decrease of the equilibrium plateau pressure of the elaborated nanocomposite material following the relation:

$$\ln(P_{H_2}) = \frac{\Delta G_T^0}{RT}.$$

5. Conclusion

The milling duration relative to the formation of the Mg_2Ni phase, reported in the literature, range from 22 [5] to 100 h [7]. In this work, the following conclusions can be easily established:

- We have successfully elaborated Mg_2Ni rich nanocomposite materials, with some residual Ni and moderate proportions of an amorphous phase, within 4 h alloying duration for 10 W g^{-1} injected shock power and within 18 h alloying duration for 3.5 W g^{-1} injected shock power.
- The optimal hydrogen absorption capacity namely 3.53 wt.% (3.75 H $mole^{-1}$), is reported for the S_{VII} sample synthesized at an injected shock power of 3.5 W g^{-1}.
- After 4 h milling at 10 W g^{-1}, we obtained a capacity as high as 3.25 wt.% (hydrogen desorption capacities of 3.2 wt.% are reported in Refs. [7,3]). So, we also elaborated, with smaller alloying duration, some Mg–Ni nanocomposite materials exhibiting similar or better hydrogen absorption–desorption properties than those reported in Refs. [3,5,7].

References

[1] X.-L. Wang, N. Haraikawa, S. Suda, J. Alloys Comp. 231 (1995) 397–402.
[2] H. Itoh, O. Yochinari, K. Tanaka, J. Alloys Comp. 231 (1995) 483–487.
[3] M.Y. Song, J. Mater. Sci. 30 (1995) 1343–1351.
[4] K. Tokumitsi, Z. Phys. Chem. 183 (1994) S443–S452.
[5] J.H. Huot, E. Akiba, T. Takada, J. Alloys Comp. 231 (1995) 815–819.
[6] D. Sun, Y. Lei, W. Liu, J. Jiang, J. Wu, Q. Wang, J. Alloys Comp. 231 (1995) 621–624.
[7] A.K. Singh, A.K. Singh, O.N. Srivastava, J. Alloys Comp. 227 (1995) 63–68.
[8] S. Orimo, H. Fujii, K. Ikeda, Acta Mater. 45 (1997) 331.
[9] L. Zaluski, A. Zalska, J.O. Strom-Olsen, J. Alloys Comp. 253–254 (1997) 70.
[10] M. Abdellaoui, E. Gaffet, J. Alloys Comp. 209 (1994) 351–361.
[11] A. Antoniadis, J. Berruyer, A. Filhol, Int. Rep. 87AN22T, Institut Lauë Langevin, Grenoble, 1988.
[12] M. Abdellaoui, T. Barradi, E. Gaffet, J. Alloys Comp. 198 (1993) 155–164.
[13] M. Abdellaoui, E. Gaffet, T. Barradi, F. Faudot, IEEE Trans. Magn. 30 (6) (1994) 4887–4889.
[14] M. Abdellaoui, E. Gaffet, C. Djega-Mariadassou, Mater. Sci. Forum 179–181 (1995) 109–114.
[15] E. Gaffet, M. Abdellaoui, N. Malhouroux, Mater. Trans. JIM 36 (2) (1995) 198–209.
[16] E. Gaffet, N. Malhouroux, M. Abdellaoui, J. Alloys Comp. 194 (1993) 339–360.
[17] E. Gaffet, M. Harmelin, J. Less-Common Metals 157 (1990) 201–222.
[18] G. Cocco, S. Enzo, S. Schiffini, L. Battezzati, Mater. Sci. Eng. 97 (1988) 43–46.
[19] M. Abdellaoui, E. Gaffet, Acta Metall. Mater. 43 (3) (1995) 1087–1098.
[20] M. Abdellaoui, J. Alloys Comp. 264 (1998) 285–292.
[21] M. Abdellaoui, D. Cracco, A. Percheron-Guegan, J. Alloys Comp. 268 (1998) 233–240.